STUDY OF THE MARS THERMOSPHERIC TEMPERATURES DURING THE SOUTHERN POLAR WINTER.

F. González-Galindo, M.A. López-Valverde, A. Cala-Hurtado, *Instituto de Astrofísica de Andalucía-CSIC, Granada, Spain. (ggalindo@iaa.es)*, **E. Millour, F. Forget,** *Laboratoire de Météorologie Dynamique-IPSL, Paris, France*.

Introduction

The high latitudes of Mars are the most elusive regions to observations. This is particularly true during the polar winter, when the poles are in full darkness during an extended period of time. However, the polar regions are home to a number of processes that strongly influence the whole climate of the planet, as CO2 condensation/sublimation and cloud formation, to name a few. A good knowledge of these regions is thus essential, and models need to be used to complement and "fill the gaps" in the data coverage.

Focusing on the upper atmosphere (mesosphere / thermosphere), the observations have unveiled interesting phenomena. Aerobraking measurements found an intense polar warming in the lower thermosphere during Northern winter, but no warming or weak warming during Southern winter (Bougher et al., 2006; Forget et al., 2009). Intense NO nightglow emissions are predicted to occur during the polar night due to a strong transport towards the poles, but could not be detected by Mars Express SPICAM (Gagné et al., 2013). Recent MAVEN/IUVS measurements during perihelion, although not including the polar region, confirm the predicted increase of the emission when approaching the polar night. However, the IUVS observed NO nightglow emissions at this season are significantly more intense than predicted (Stiepen et al., 2016).

Here we study the temperature variability in the Martian upper atmosphere focusing mostly on the Southern polar night. A previous study of the simulated exobase temperature variability during 8 Martian Years (MYs) allowed to identify a period of very cold temperatures during the Southern polar night, followed by an intense polar warming (González-Galindo et al., 2015). This situation repeated in all the simulated years, but while the cold temperatures were little affected by interannual variability, the intensity of the polar warming was. Our aim here is to study in detail these features, to better understand their nature and origin.

Methodology

We use for this study the same simulations than in González-Galindo et al., 2015. The simulations were performed with the Mars Global Climate Model developed at the Laboratoire de Météorolodie Dynamique (LMD-MGCM) in its ground-to-exobase configuration (Forget et al., 1999; Gonzalez-Galindo et al., 2009, 2013, 2015). An improved parameterization of the 15 μm cooling and a procedure to take into account the day-to-day variability of the UV solar flux are included in this version of the model. The dust opacities from Montabone et al., (2015), including interannual variability, are also used here.

Results

Figure 1 shows the temporal variability of the noon temperatures at the exobase level (namely the 10^{-6} Pa pressure level) at latitude 80S for all the simulated Martian Years (MY24 to MY32). A similar pattern is obtained in all the other years: temperatures decrease during the first part of the year until reaching a minimum level in the period Ls=40-60. This temperature decrease is produced by the progressive reduction in the radiative heating of the upper atmosphere when approaching the polar night. The minimum temperatures are close to 120 K, with little interannual variability (around 10-15 K). These are very low values, similar to those expected in the mesopause and to those observed in the so-called Venus upper atmosphere "cryosphere". A strong and sudden increase of temperature is produced around Ls=60-70 for all MYs. This increase can be as strong as 100 K, and spans just a few sols, although with significant interannual differences in the precise timing, intensity and duration of this sudden temperature increase. Temperatures then remain relatively high during a significant period of time, to start decreasing after about Ls=90 and to reach a second minimum of about 140 K around Ls=120.

Note that at these latitudes there is no solar illumination at Ls≈60, which indicates a dynamical origin of this warming. Previous modeling studies of the thermospheric polar warming during Northern winter attributed its presence to a mixture of intense global circulation, insitu tides and gravity waves (Bougher et al., 2006; Bell et al., 2007; González-Galindo et al., 2009b; Medvedev et al., 2011).

Next we analyze We now study in more detail one of the years, MY26. The vertical and latitudinal structure of the simulated temperature at Ls=50 (within the period of minimum temperaturtes) and at Ls=80 can be seen in Figs. 2 and 3, respectively.

For the Ls=50 case the latitudinal variation in the up-

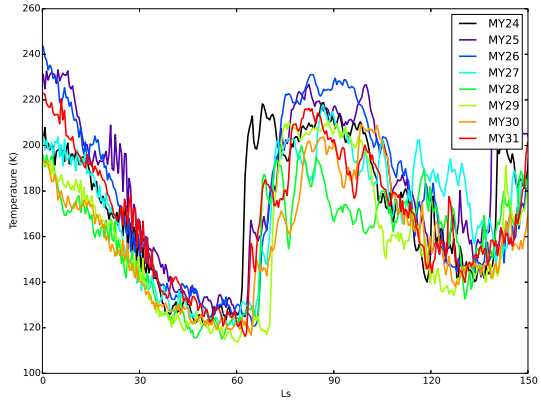

Figure 1: Noon temperatures at the exobase and latitude 80S, simulated for 8 MYs

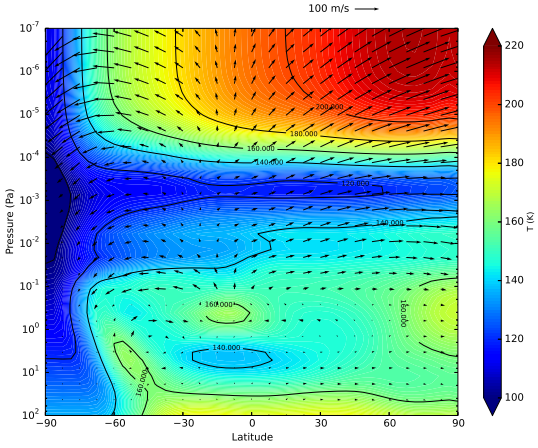

Figure 2: Lat-pressure slice of the noon temperatures for MY26, at Ls=50

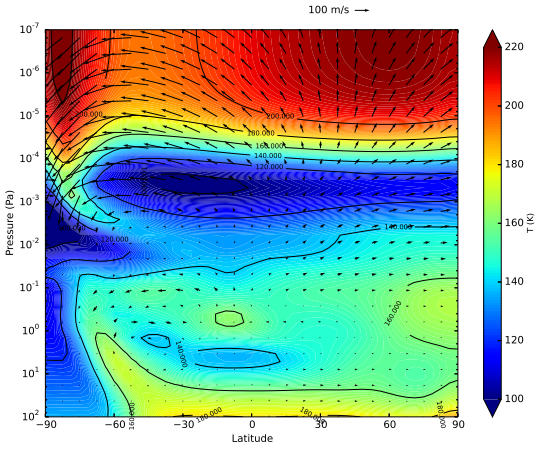

Figure 3: As Fig. 2, but for Ls=80

per atmosphere is, to first order, what could be expected from radiative equilibrium considerations: maximum temperatures (around 210 K) in the summer (Northern) hemisphere, and temperatures decreasing when approaching the winter (Southern) polar regions down to a minimum of about 115K. Note that this is also the case for the mesopause (around P=10^{-3} Pa), although with a much smaller gradient, with temperatures going from about 130 K in the summer pole to less than 100 K in the winter pole. Regarding the wind structure, thermospheric meridional winds are basically northwards in the Northern hemisphere and southward in the Southern hemisphere, with ascent of air everywhere at low and mid latitudes. The zonal winds (not shown) above the 0.1 Pa pressure level are eastward in the Southern hemisphere and westward in the Northern hemisphere. The most salient feature is a strong eastward jet spanning the whole upper atmosphere in the Southern hemisphere, with maximum wind speed of about 180 m/s at Lat=75S, while the westward winds in the Northern hemisphere are significantly weaker, with a maximum of about 80 m/s in the mid latitudes. This jet limits and defines a clear polar vortex.

At Ls=80, while the situation in the lower atmosphere (layers below 0.1 Pa) is basically the same than at Ls=50, dramatic changes in the upper atmosphere ocurred near the winter pole. In the whole winter hemisphere the thermospheric temperatures increased with respect to Ls=50, particularly in mid and high latitudes. A maximum temperature of 225 K is now obtained close to the winter pole, with a strong gradient from lat≈30S. Meridional winds are now directed towards the Southern (winter) hemisphere southward of 30N, with a significant increase of the wind intensities with respect to Ls=50, particularly close to the pole. Also the vertical downward winds are strongly enhanced in the polar region. This produces an increase of temperature in a "tongue" of air around the mesopause extending from about 80S to 60S. For the zonal winds, the westward jet in the Northern hemisphere has significantly grown in horizontal extension and intensity. Winds are now westward everywhere except in the high latitudes of the Southern hemisphere, and the maximum wind intensity exceeds 200 m/s close to the equator. On the other hand, the eastward jet is now confined to lat<60S, and its maximum intensity is reduced to about 110 m/s.

All these results indicate a strong and sudden change in the global circulation that induces a strong warming of the polar winter region. This thermospheric polar warming during the Southern winter seems to be a robust feature of the model, which is consistently predicted independently of the solar activity and of the dust load. However, the observations are not very conclusive with respect to the presence of the polar warming at this season. The temperatures at 120 km derived from MGS aerobraking do not seem to present any polar warming

(Bougher et al., 2006). The analysis of SPICAM stellar occultations (Forget et al., 2009) during the period Ls=120-150 shows a polar warming at altitudes below the mesopause, but is not conclusive at higher layers due to the spread of the data. We will discuss different possibilities to explain this apparent data-model discrepancy.

Acknowledgements

This work has received funding from the European Union's Horizon 2020 Programme (H2020 - Compet - 08 - 2014) under grant agreement UPWARDS-633127. ACH has been funded by CSIC intramural contrat 201450E022 and the rest of the Spanish team has been supported by ESP2015-65064-C2-1-P (MINECO/FEDER)

References

Bell, J. M., S. W. Bougher, and J. R. Murphy (2007). Vertical dust mixing and the interannual variations in the Mars thermosphere, J. Geophys. Res., 112, E12002.

Bougher, S. W., J. M. Bell, J. R. Murphy, M. A. Lopez-Valverde, and P. G. Withers (2006), Polar warming in the Mars thermosphere: Seasonal variations owing to changing insolation and dust distributions, Geophys. Res. Lett., 33, L02203, doi:10.1029/2005GL024059

Forget, F., F. Hourdin, R. Fournier, C. Hourdin, O. Talagrand, M. Collins, S. R. Lewis, P. L. Read, and J.-P. Huot (1999). Improved general circulation models of the Martian atmosphere from the surface to above 80 km, J. Geophys. Res., 104, 24,155-24,176

Forget, F., F. Montmessin, J.-L. Bertaux, F. González-Galindo, S. Lebonnois, E. Quémerais, A. Reberac, E. Dimarells, and M. A. López-Valverde (2009). Density and temperatures of the upper Martian atmosphere measured by stellar occultations with Mars Express SPICAM, J. Geophys. Res., 114, E01004.

Gagné, M.-E., J.-L. Bertaux, F. González-Galindo, S. M. L. Melo, F. Montmessin, and K. Strong (2013). New nitric oxide (NO) nightglow measurements with SPICAM/MEx as a tracer of Mars upper atmosphere circulation and comparison with LMD-MGCM model prediction: Evidence for asymmetric hemispheres, J. Geophys. Res. Planets, 118.

González-Galindo, F., F. Forget, M. A. López-Valverde, M. Angelats i Coll, and E. Millour (2009a). A ground-to-exosphere Martian general circulation model: 1. Seasonal, diurnal, and solar cycle variation of thermospheric temperatures, J. Geophys. Res., 114, E04001.

González-Galindo, F., F. Forget, M. A. López-Valverde, and M. Angelats i Coll (2009b), A ground-to-exosphere Martian general circulation model: 2. Atmosphere during solstice conditions. Thermospheric polar warming, J. Geophys. Res., 114, E08004.

González-Galindo, F., J.-Y. Chaufray, M. A. López-Valverde, G. Gilli, F. Forget, F. Leblanc, R. Modolo, S. Hess, and M. Yagi (2013). Three-dimensional Martian ionosphere model: I. The photochemical ionosphere below 180 km, J. Geophys. Res. Planets, 118.

González-Galindo, F., M. A. López-Valverde, F. Forget, M. García-Comas, E. Millour, and L. Montabone (2015). Variability of the Martian thermosphere during eight Martian years as simulated by a ground-to-exosphere global circulation model, J. Geophys. Res. Planets, 120, 2020-2035, doi:10.1002/2015JE004925.

Medvedev, A. S., E. YiÄit, P. Hartogh, and E. Becker (2011). Influence of gravity waves on the Martian atmosphere: General circulation modeling, J. Geophys. Res., 116, E10004, doi:10.1029/2011JE003848.

Montabone, L., F. Forget, E. Millour, R.J. Wilson, S.R. Lewis, B. Cantor, D. Kass, A. KleinbÃ¶hl, M.T. Lemmon, M.D. Smith, and M.J. Wolff (2015). Eight-year Climatology of Dust Optical Depth on Mars, Icarus, doi: http://dx.doi.org/10.1016/j.icarus.2014.12.034

Stiepen, A., A.I.F. Stewart, S.K. Jain, N.M. Schneider, J.I. Deighan, F. González-Galindo, J.-C. Gérard, M.H. Stevens, S.W. Bougher, Z. Milby, J.S. Evans, M.S. Chaffin, W.E. McClintock, J.T. Clarke, G.M. Holsclaw, F. Montmessin, F. Lefevre, D.Y. Lo, B. Hubert, and B.M. Jakosky (2016). Nitric Oxide Nightglow and inter-hemispheric transport at Mars mesosphere from MAVEN/IUVS observations, paper submitted to J. Geophys. Res.